Advanced Nano Research
Volume 3, Issue 1, pp. 28-39, 2020
DOI: https://doi.org/10.21467/anr.3.1.28-39
ISSN: 2581-5164
RESEARCH ARTICLE

Solubility of Mn in ZnO Crystallites Synthesized Using Solid State Techniques

Esau Nii Abekah Akwetey Armah[1, 2,3*], Martin Egblewogbe[2], Hubert Azoda Koffi[2], Alfred Ato Yankson [2], Francis Kofi Ampong[1], Francis Boakye[1], Josef Kwaku Ametefee Amuzu[2], Robert Kwame Nkum[1]

[1] Department of Physics, Kwame Nkrumah University of Science and Technology, Ghana
[2] Department of Physics, LG 63, University of Ghana, Legon, Accra, Ghana
[3] Foundation Department, Lancaster University Ghana, P. O. Box CT9823, Cantonments, Accra, Ghana

[*] Corresponding author email: akweteyniiabekah@gmail.com

Received: 17 June 2020 / Revised: 11 September 2020 / Accepted: 28 September 2020 / Published: 30 September 2020

ABSTRACT

Powder samples of $Zn_{1-x}Mn_xO$ nanocrystal were synthesized at a temperature of 200 °C using solid phase method. Dopant concentrations of $0.005 \leq x \leq 0.5$ were studied. Powder x-ray diffraction (PXRD) patterns of the samples were analyzed with a view of determining the onset of secondary phases, hence the solubility limit of the dopant. The solubility limit for Mn in ZnO samples synthesized at 200 °C is realized at $x < 0.3$. With a regular pattern in increment of the Mn concentration, there were variations observed in the trend of the relative intensity, 2θ position and d-spacing indicating uneven addition of Mn (thus Mn^{2+}, Mn^{3+} or Mn^{4+}).

Keywords: Doping Concentration, Solid Phase, Solubility Limit

1 Introduction

Oxides, particularly of the transition metals, constitute a very important material class, displaying many important properties and participating in a variety of functions. Because of the high oxygen content of earth's atmosphere, oxides are also some of the most stable materials formed. Many transition metal oxides, particularly those of the early transition metals, are often biocompatible, or at least, not very toxic. This is perhaps the single greatest advantage of oxide materials [1].

Materials exhibiting transparency and electrical conductivity concurrently are termed transparent conductors (TCs) and materials used for this purpose are mostly oxide based hence the term transparent conducting oxides (TCOs) [2]. TCO's are usually wide band gap materials which have high carrier concentration. This higher concentration of carriers is a result of defects in the material or extrinsic dopants [3, 4]. These oxide compounds are extensively used in manufacturing photovoltaic cells, flat screen display panels, electrochromic devices, transparent electronics and sensors [5]. In optimizing the function of TCOs, an elevated temperature during deposition or annealing is generally required at some point in their fabrication. Heat-sensitive substrates such as plastics are limited to temperature below 200 °C and glass substrates are limited to a temperature of 250 °C. If the temperature is increased above 250 °C, the possibility of inter diffusion layers occurring becomes high, thereby damaging the device performance [6].

Research has shown that, substitution of a fraction of the original atoms of the lattice of ZnO host by one of the transition metal (TM) ions especially, Mn, Co, Fe, and Cr and Ni, in appropriate concentrations in the host material, could introduce ferromagnetic properties while its semiconducting property is retained making the material a dilute magnetic semiconductor (DMS). By combining both semiconducting and ferromagnetic properties, DMS can lead to spintronic devices that use both spin and charge of electrons [7, 8]. Mn has the advantage of being used as a dopant because of its high magnetic moment and the relatively small ionic radii difference between Mn^{2+} and Zn^{2+} which facilitates its incorporation into the

ZnO lattice. Though countless efforts have been undertaken to examine the role of dopants in ZnO, Mn-doped ZnO has become tremendously a vital material for its co existing magnetic, semiconducting and optical properties [9]. It has been employed as a material for the fabrication of solar cells, transparent electrodes, gas sensors, etc. [10].

The need to develop eco-friendly synthesis procedures for the production of nanoparticles arises as a result of recent nanotechnology research. Synthesis procedures are either expensive or they produce environmental pollutants. Another challenge associated with such synthesis procedures is the cost of energy due to heating for a long period of time and the need to work at very high temperatures. The chemical route for synthesizing nanomaterials at low temperature provides excellent control over metastable phases, uniform homogeneity, particle sizes and morphologies of the synthesized nanomaterials [11].

During the past decades, several techniques have been used in doping ZnO with transitional metals, especially manganese to investigate its electrical, optical, magnetic and other properties. Mn doped ZnO have been synthesized by various wet (liquid) and dry (solid-state reaction) techniques. For the above properties to be achieved, an adequate concentration of doping atoms has to be incorporated into the mother crystal. However, for efficient doping, the incorporation of the dopant must not cause a structural change in the host atom [12]. Different doping techniques can achieve different solubility limits. However, other functional properties approach a limit where the additional introduced dopant atoms cease to generate extra free carriers but rather cause structural distortion [13]. Although solid state reaction method is known to be simple and reproducible, only few reports were devoted to the study of Mn doped ZnO nanoparticles using this method.

In the solid-state reaction, different routes have been adopted. However, in almost all of the cases, already prepared or purchased ZnO and oxides of Mn were used as precursors according to the required compositions and ground to obtain homogeneous mixtures for preparation of the sample. The resulting powders were heated at temperatures ranging between 400 °C and 1400 °C for a period of time between 8 h and 24 h. Such work has been reported by many researchers.

For instance, using the solid state reaction, Lançon et al [14] synthesized Mn-doped ZnO by grinding the mixture of Mn carbonate and ZnO and annealing at 400 °C. From careful analysis of the XRD patterns, MnO was found to be presence in the sample. The solid-state reaction route was also used by Marquina et al [15] to prepare Mn-ZnO at 2% doping from high-purity powders of ZnO and MnO_2, which were mixed together, ground and calcined at 500 and 900 °C for 12 h. From the X-ray diffraction results, one known phase present in small quantities was readily identified as Mn_2O_3.

Ahmed [16] in determining the structural, optical, and magnetic properties of Mn-doped ZnO used the appropriate amounts of ZnO and MnO_2 according to the required compositions (2%, 4% and 8%) to prepare the samples by the standard solid-state reaction route. In preparing the samples, the precursors were ground to obtain homogeneous mixtures and heated at 400 °C for 8 h in air. The resulting powder was reground, pressed into dense pellets and sintered at 500 °C in air for 12 h and finally ground to obtain the nano powder samples. From the XRD spectra an additional secondary phase was observed at 33° in all the samples in addition to the dominant hexagonal peaks of ZnO. At 8% doping concentration, two additional peaks evolve at 38.27° and 55.21°, corresponding to Mn_2O_3 impurity phase. The intensity of these impurity phases increased as the Mn-doping increased. A careful analysis of the XRD peak positions indicates a slight shifting of the diffraction peaks towards a lower angle with Mn-doping. However, lattice parameters and cell volume increased with a Mn addition up to 4% but decreased at 8% doping concentration. These suggest the incorporation of Mn ions into the lattice of the hexagonal wurtzite structure of the ZnO.

In the work of Mobarak et al [17], MnO and PbO doped ZnO nanoceramic was synthesized by solid state reaction method using 1%, 1.5%, 2.0% and 2.5% of the various dopants. In synthesizing the samples, powders of MnO, PbO and ZnO were ground in the appropriate ratio and ball milled. The resultant powder was made into pellets form and oven dried and calcinated at 850 °C, 1000 °C and 1050 °C in air for 8 h.

The XRD studies reveals a single-phase hexagonal wurtzite structure of the samples without any other intermediate phases.

Bilgili [18] uses the solid state method to dope ZnO with 1% and 5% Mn. During the synthesis, the appropriate amount of ZnO and Mn_2O_3 powders were ground and calcined for 8 h at 450 °C. The products were then reground and pressed into pellets form and again sintered at 900 °C for 12 h. The XRD results revealed hexagonal wurtzite structure corresponding to ZnO without any impurity or secondary phases. It was also observed that, with increasing Mn concentrations, the intensity of the diffraction increased, the position of the peaks shifted towards lower angles and the lattice parameters increased at the initial 1% doping. However, as the doping concentration is increased from 1% to 5%, there was slight decrease in the lattice parameters.

In co-doping ZnO using the solid state method in order to investigate the relationship between the band gap and the refractive index, Senol et al [19] used 1% of Cu and up to 5% of Mn as the dopants. In the preparation of the nanoparticles, acetates of the precursors in the appropriate mass were grounded and heated at temperature of 600 °C for 2 h. During the structural characterization using XRD, hexagonal wurtzite structure of ZnO was observed as the main phase with Mn_2O_3 as an additional secondary phase. Fluctuations in the lattice parameters were observed due to the presence of the Mn and Cu ions replacing Zn ions in the lattice having different ionic radii.

To investigate the microstructure and magnetic properties of Mn doped ZnO by Sebayang et al [20] using the solid-state reaction method, powders of ZnO and Mn were used with doping concentration of 5% and 9%. In the synthesis, the precursors were first wet milled for 3 h using high-energy milling and dried in ambient air at 100 °C for 1 h. The resulting dried powder was hot pressed into pellets and dried again at 150 °C. The XRD results showed a single-phase polycrystalline hexagonal wurtzite structure of ZnO with no secondary phase. It was observed that the peak intensity of reflection from the (002) plane for Mn doped ZnO nanoparticles was lower than that of the undoped ZnO. Also, peaks of the Mn doped ZnO nanoparticles were found to have shifted to higher angles.

Thus, to the best of our knowledge, Mn-doped ZnO nanoparticles without post heat treatment or annealing have rarely been investigated. Therefore, we seek to develop a very simple and environmentally friendly synthesis technique to produce both pure and Mn-doped ZnO nanoparticles. Thus, the focus of this study is the development of an environmentally friendly synthesis route for growing Mn-doped ZnO nanocrystals by the solid phase method. The objective is to develop a solid phase method of doping ZnO with Mn, using lower temperatures without washing of the nanocrystals and short growth duration compared with what has been reported in the literature.

2 Experimental Procedures

2.1 Synthesis of Mn Doped ZnO Nanocrystals

In this procedure, yellowish crystals of ZnO_2 were first prepared using the wet chemical process as described earlier in full details in the work of Armah et al [21]. The appropriate amounts of already prepared ZnO_2 and manganese acetate were ground in order to achieve uniform mixture of the precursors using the required composition. After adding the manganese acetate, the yellowish crystals became brown. The powder was then transferred to a beaker and placed on a hot plate at a temperature of 120 °C and gradually increased to 200 °C in 10 minutes. This temperature was maintained for 3 hours. The temperature of 200 °C was chosen based on the previous experiment where ZnO was doped with Mn using the wet chemical synthesis method. This process was repeated for all the doping concentration ($0.005 \leq x \leq 0.5$) and the colour of the crystals was observed to become darker as the dopant concentration increased. The overall processing time used in order to get the sample fully dried and obtain the desired crystal phase to ensure good crystallinity was 4 hours.

The flowchart for the synthesis of manganese doped ZnO nanoparticles by solid state reaction method is shown in figure 1. The reaction taking place during preparation of the doped ZnO nanoparticles is:

$$ZnO_2 + xMn\,(CH_3COO)_2.\,6H_2O \rightarrow Zn_{1-x}Mn_xO + 2CH_3COO + 6H_2O + 1/2O_2$$

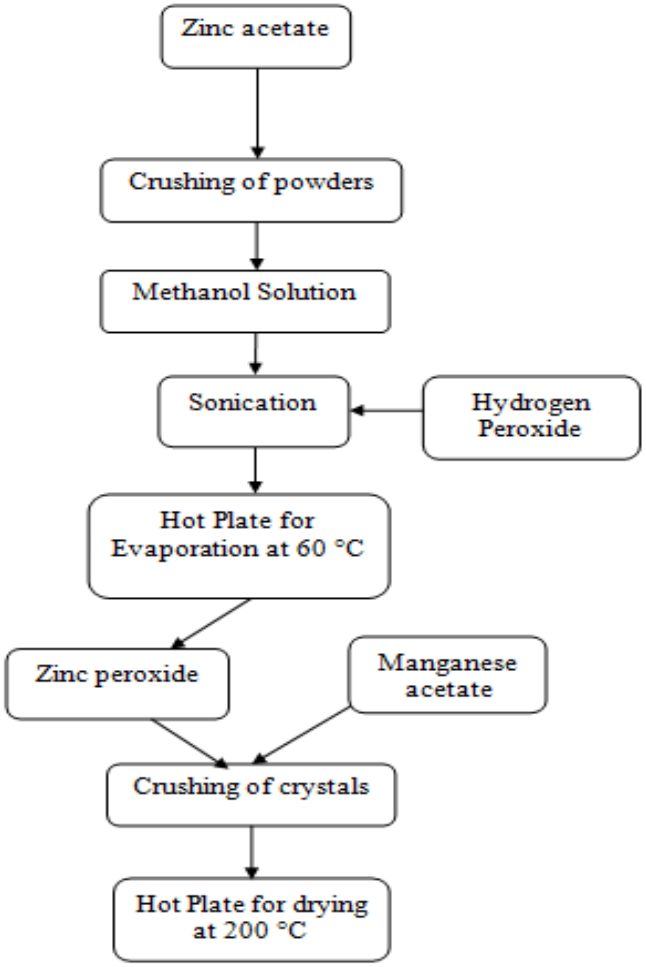

Figure 1: *Flow Chart for the synthesis of Mn doped ZnO using the solid state method*

2.2 Characterization

The characterization of the Mn-doped ZnO nanocrystal samples was carried out using a PANalytical X-ray powder diffractometer with the CuKα line at λ = 1.54056 x10^{-10} m. The scan parameters were 2θ scanning range from 20° to 70° with a step size of 0.0060 and scan step time of 0.7 seconds and measuring temperature of 25 °C.

3 Results and Discussion

Figures 2 to 11 show diffractograms of Mn doped ZnO nanoparticles synthesized by solid phase method at a temperature of 200 °C with Mn doping concentration composition of between 0.5% and 50%. The characteristic peaks indexed to the (100), (002), (101), (102), (110), (103) and (112) planes show crystalline features which matched with the ICSD card numbers 01-078-2585 and 01-089-7102 respectively. The analysis of the diffraction peaks revealed the presence of mainly wurtzite (hexagonal) structural phase similar to pure ZnO in all the compositions studied.

The XRD patterns of the samples up to 20% show that there were no additional secondary peaks due to Mn incorporation as shown in Figures 2 to 9. The samples maintained good crystallinity of doping, which confirmed the proper phase formation of the materials. This also reveals that Mn is successfully doped in ZnO. However, a shift of the peak positions was observed with the introduction of the Mn doping

percentages. This is due to the change in the lattice constants of the hexagonal ZnO structure due to the Mn incorporation. The compound identified by the XRD at 0.5% doping concentration was only ZnO. Between 1% and 20%, the compounds identified were both manganese zinc oxide and ZnO. This is because the possible remaining impurities from the synthesis of zinc peroxide by the wet chemical method could be zinc hydroxide and un-reacted acetates which decomposes at temperatures above 120 °C and releases oxygen to form zinc oxide [4]. At these levels of doping the sample does not show traces of Mn compounds such as $MnCO_3$, Mn_2O_3, MnO or MnO_2.

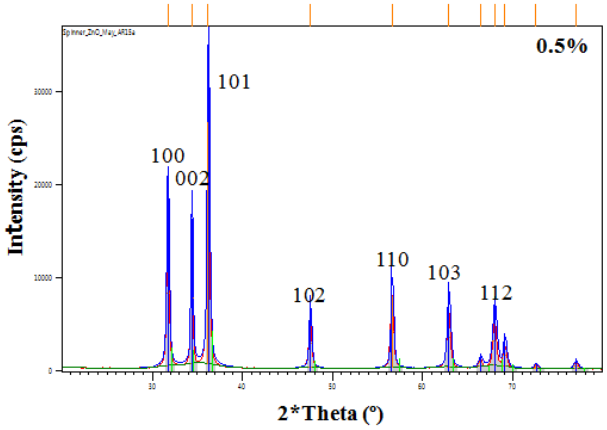

Figure 2: *XRD pattern for $Zn_{1-x}Mn_xO$ at x= 0.5%*

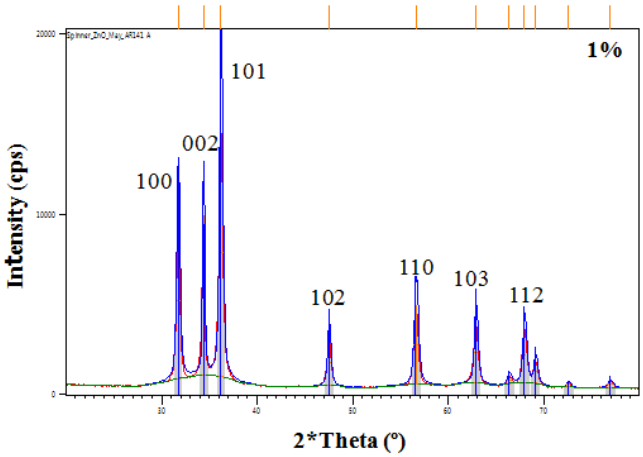

Figure 3: *XRD pattern for $Zn_{1-x}Mn_xO$ at x= 1%*

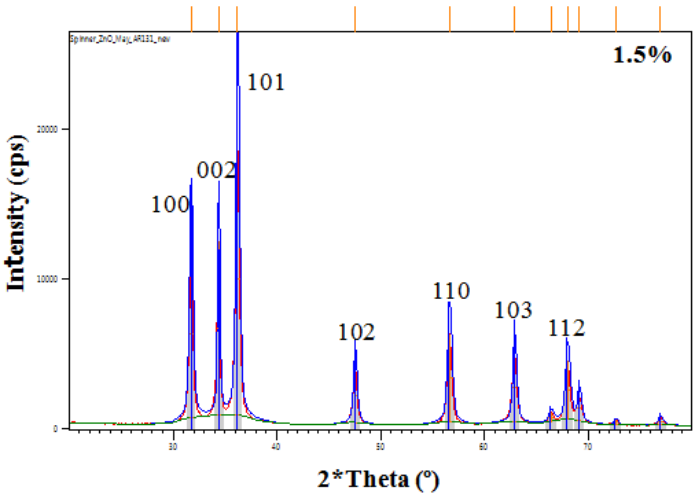

Figure 4: *XRD pattern for $Zn_{1-x}Mn_xO$ at x= 1.5%*

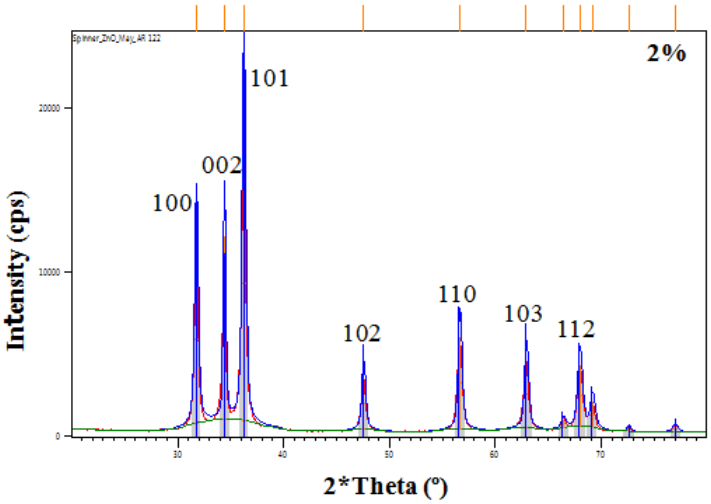

Figure 5: *XRD pattern for $Zn_{1-x}Mn_xO$ at x= 2%*

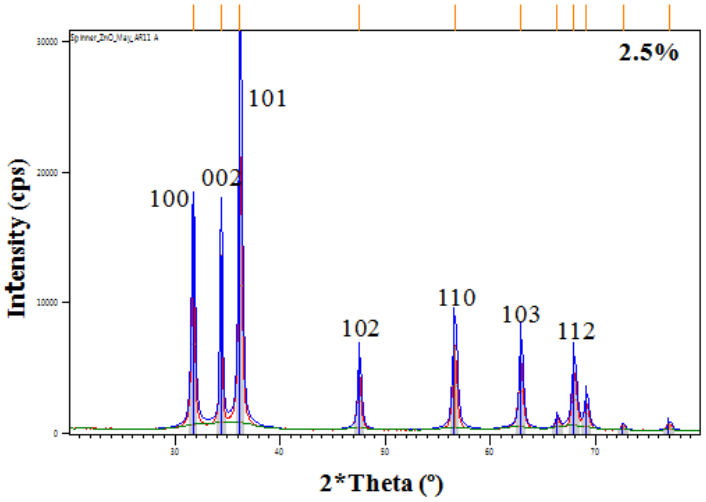

Figure 6: *XRD pattern for $Zn_{1-x}Mn_xO$ at x= 2.5%*

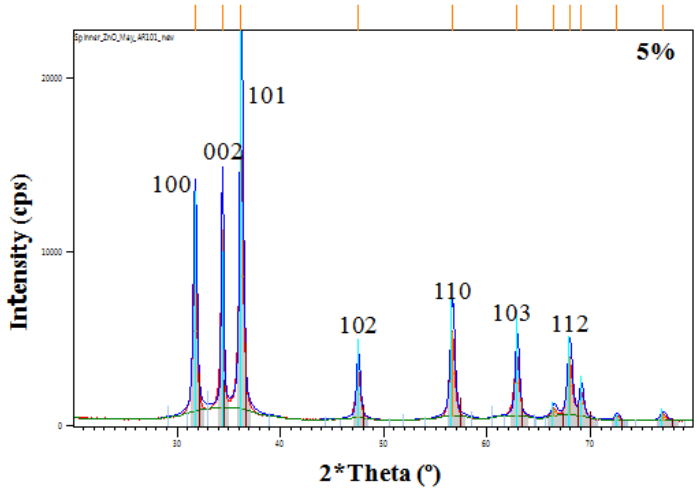

Figure 7: *XRD pattern for $Zn_{1-x}Mn_xO$ at x= 5%*

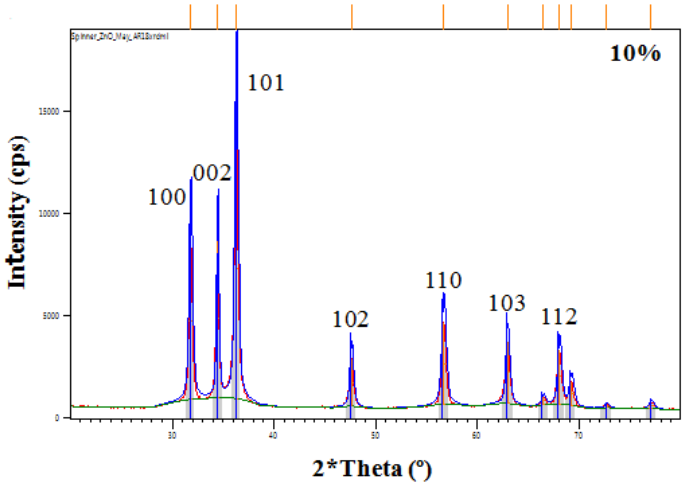

Figure 8: *XRD pattern for $Zn_{1-x}Mn_xO$ at x= 10%*

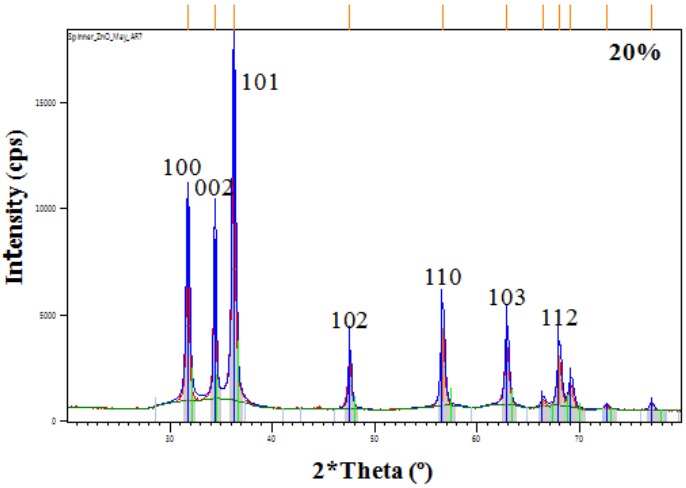

Figure 9: *XRD pattern for $Zn_{1-x}Mn_xO$ at x= 20%*

At 30% doping concentration, for the first time, in addition to the dominant hexagonal-$Zn_{1-x}Mn_xO$ phase, two tiny peaks of an additional secondary phase labelled (x) at 29.20° and 44.44° were observed in the XRD spectra, which are indicated in Figure 10 which is also reported by Ahmed [16]. These could be due to impurity phase, and are indexed to Mn_3O_4 based on the diffractogram.

After the 30% doping concentration the number of secondary peaks increased gradually. The number of these peaks as well as their intensities increased as the dopant concentration was increased (Figures 11 and 12). The XRD lines for the 40% sample show five additional peaks at 29.24°, 32.93°, 44.59°, 58.74° and 60.64° (Figure 11) and at 50% doping six additional peaks were observed at approximately 29.14°, 32.74°, 44.70°, 58.87°, 60.53° and 64.95° (Figure 12). The Mn_3O_4 impurity phase peak observed at 30% also appears in the 40% and 50% samples along with the dominant hexagonal-$Zn_{1-x}Mn_xO$ in addition to Mn_2O_3 and zinc carbonate hydroxide ($Zn_4CO_3(OH)_6.2H_2O$) were also identified based on the diffractogram. It is important to note that, adversely, excessive Mn doping encouraged spinel formation such as $ZnMnO_3$ and $ZnMn_3O_7$ that could lead to poor non-linearity. However, during heating, the solubility of Mn ions could increase because of Mn^{2+} reduction to Mn^{3+} or Mn^{4+} [22].

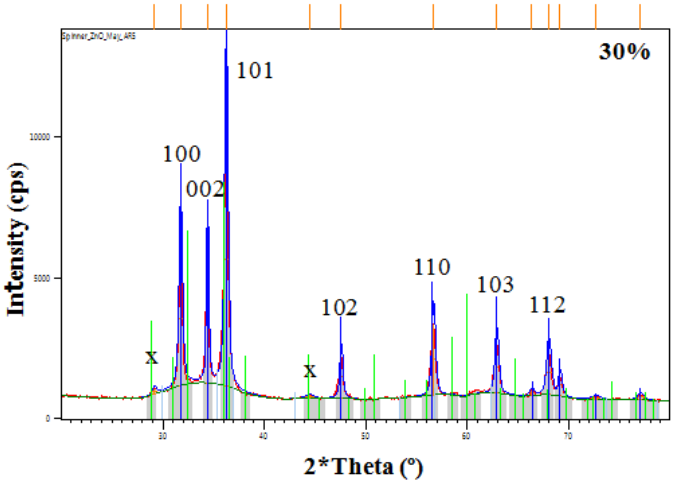

Figure 10: *XRD pattern for Zn1-xMnxO at x= 30%*

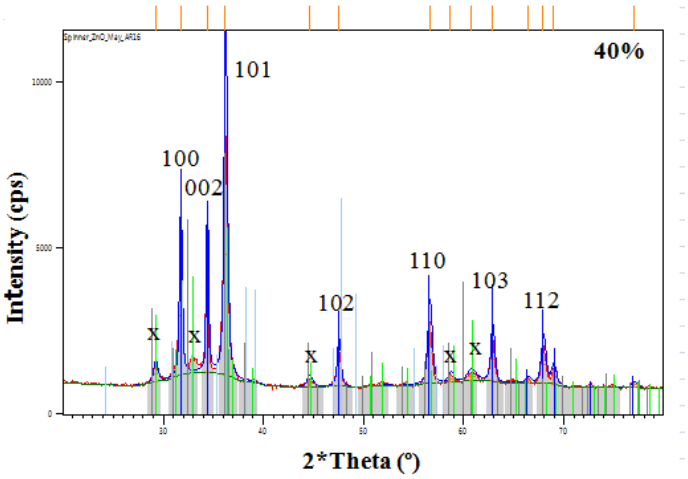

Figure 11: *XRD pattern for Zn1-xMnxO at x= 40%*

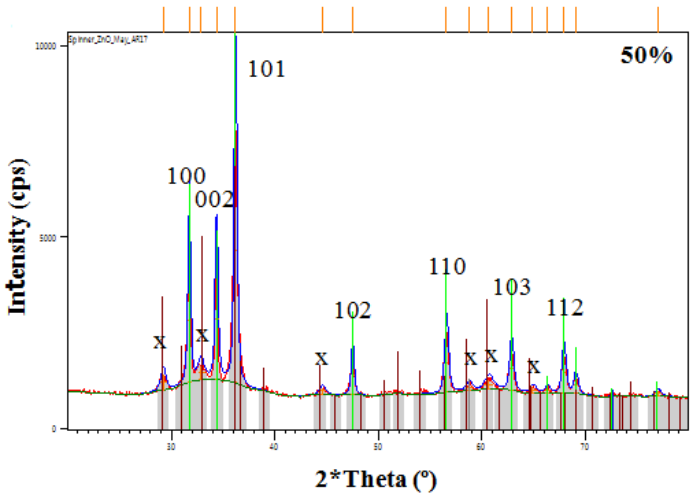

Figure 12: *XRD pattern for Zn1-xMnxO at x= 50%*

The presence of the additional secondary phases as indicated by these peaks is thought to be the result of manganese acetate residue in the sample (and is probably in the form MnO, MnO_2, Mn_2O_3 or Mn_3O_4) [23-25]. The absence of the impurity peaks implies that the percentage doping employed is within the solubility

limits of Mn in ZnO with respect to the corresponding temperature. It could be assumed that the Mn ion has substituted the Zn site without changing the wurtzite structure.

From the diffractograms, it was observed that, the changes in the relative intensity, 2θ position and d-spacing were noticed in the reflections from the (100) and (002) planes. The relative intensities of the XRD peaks were observed to vary with different doping concentrations. This was realized when the three most prominent peaks indexed by the XRD at (100), (002), (101) planes were compared. The most striking feature is that, for all the samples with different doping concentrations, the diffraction peak at (101) plane was found to be the most prominent with relative intensities of 100% whiles that of (100) and (002) planes varies between 45% and 70%. Interestingly, all the observed peaks correspond very well to wurtzite Mn doped ZnO [26-28]. In the event where no additional peaks are observed, which might belong to Mn related secondary phases, it may be suggested that, Mn atoms are located at substitutional sites within the ZnO structure. This is also supported by Shatnawi et al [8].

The changes in the relative intensity as doping concentration is increase was irregular. Similarly, between the reference planes of (100) and (002), the changes in the relative intensity was irregular. For instance, at 0%, the relative intensity of the (002) plane is higher than that of the (100) plane (68.58 and 61.68 respectively) and at 0.5%, the relative intensity of the (100) plane is higher than that of the (002) plane (59.64 and 53.88 respectively). This trend is observed for the rest of the doping concentrations. In all, the 50% doping has the lowest relative intensity (47.36 and 45.77 for (100) and (002) planes respectively), but generally, the relative intensity decrease as doping concentration is increased.

A careful analysis of the XRD peak positions indicates a slight shifting of the diffraction peaks in the 2θ position with Mn-doping. These shifts in peak positions in the diffraction pattern due to increasing Mn concentration have been observed to be irregular as shown in Table 1. It was observed that, as the dopant is introduced at 0.5%, the diffraction peak shift slightly from 31.8021 to 31.7482 with the (100) plane. The (002) plane also saw a shift from 34.4453 to 34.4075. Similarly, at 1%, the diffraction peak shift slightly from 31.8021 to 31.7491 with the (100) plane. The (002) plane also saw a shift from 34.4453 to 34.3930. These shows a shift to lower angles. A shift to lower angles implies that the Zn^{2+} in ZnO structure has been replaced by Mn^{2+} ion because of increase in d spacing due to substitution of lattice site by ion of higher radius. This trend continues for the rest of the doping except at 10% where there was an increase in the 2θ position from 31.8021 to 31.8272 for the (100) plane and from 34.4453 to 34.4700 for the (002) plane when compared with the undoped ZnO sample of 0% Mn. At this concentration, where the shift is towards the higher angles, it could be said that, the Zn^{2+} in ZnO structure has been replaced by Mn^{3+} and/ or Mn^{4+} ion. The shift in the XRD diffraction peaks indicates that the Mn ion is successfully incorporated into the ZnO lattice as a substitutional atom. This finding has also been reported by Armah et al [21], Abrishami et al [29] and Goswami and Singha [28]. This is most likely attributable to growth process and conditions (synthesis method phase and temperature), which allow different distributions of Mn within the ZnO structure [25]. The change in the XRD patterns (expanding or contracting of width) clearly indicates that the XRD reflections are shifted to lower or higher values with increasing concentration of Mn. This is a proof of the incorporation of Mn ions into the ZnO crystal lattice [30].

The pattern for the 2θ positions was the same for the d-spacings. Thus, at 0.5%, the d-spacings increase from 2.8139 for the (100) plane to 2.8185 and from 2.6038 to 2.6065 for the (002) plane. Also, at 1.5%, it increases to 2.8187 and 2.6076 for the (100) and (002) planes respectively. However, at 10%, d-spacings decreases from 2.8139 to 2.8117 for the (100) plane and from 2.6038 to 2.6020 for the (002) plane.

It is interesting and important to note that, the changes in the values of these parameters as doping concentration was increase were not regular with respect to the increase in dopant concentration except for the 10%. For example, the 2θ positions for the (100) plane decreased from 31.8021 at 0% to 31.7482 at 0.5%. At 1%, the values were 31.7491 which is higher than that of the 0.5%. This trend makes the trend irregular. However, these could be attributed to the fact that, the Zn^{2+} in ZnO structure might have been replaced by either Mn^{3+} and/ or Mn^{4+} ion whiles that of the 10% might be due to Mn^{2+} ion substitution.

The changes in relative intensity, 2θ position and d-spacing with different doping concentrations are tabulated in Table 1.

Table 1: *Relative intensity, 2θ position and d-spacing of prepared Mn doped ZnO nanoparticles*

Mn Doping (%)	Relative Intensity (%)		Position (°2Th)		d-spacing (Å)	
	(1 0 0) Plane	(0 0 2) Plane	(1 0 0) Plane	(0 0 2) Plane	(1 0 0) Plane	(0 0 2) Plane
0.0	61.68	68.58	31.8021	34.4453	2.8139	2.6038
0.5	59.64	53.88	31.7482	34.4075	2.8185	2.6065
1.0	62.91	64.47	31.7491	34.3930	2.8185	2.6076
1.5	62.37	63.75	31.7464	34.3929	2.8187	2.6076
2.0	61.06	66.53	31.7738	34.4187	2.8163	2.6057
2.5	58.94	61.67	31.7557	34.4093	2.8179	2.6064
5.0	60.94	67.14	31.7549	34.3971	2.8180	2.6073
10.0	60.55	60.30	31.8272	34.4700	2.8117	2.6020
20.0	57.34	57.56	31.7621	34.4089	2.8173	2.6064
30.0	52.98	54.71	31.7641	34.4118	2.8172	2.6062
40.0	49.83	52.69	31.7558	34.4064	2.8179	2.6066
50.0	47.36	45.77	31.7378	34.3676	2.8194	2.6095

From the careful analysis of the diffraction data for all the samples, a non-monotonic shift in the peak position is observed. Different Mn oxides, having Mn in different oxidation states such as Mn^{4+}, Mn^{3+} and Mn^{2+} are formed during heat treatment of Mn in oxygen. It may be noted that Mn^{4+} and Mn^{3+} have ionic radii of 0.53Å and 0.65Å, respectively, which are smaller than the ionic radius of 0.74Å for Zn^{2+} in wurtzite ZnO and also smaller than the ionic radius of 0.83 for Mn^{2+}.

Now, if Mn^{2+} ion substitutes Zn^{2+} in ZnO structure, then the XRD peaks will shift towards the lower angles because of increase in d spacing due to substitution of lattice site by ion of larger radius. However, if Mn^{3+} and Mn^{4+} go into interstitial sites, they push the surrounding atoms because their size is greater than interstitial sites. This pushing by interstitial atoms will stretch the lattice resulting in increase in the interplanar distance. On the basis of this understanding, interstitial diffusion of Mn^{3+} and Mn^{4+} in to ZnO lattice will still cause the XRD peak to shift towards the higher angles. Notwithstanding that, in this research work, it was noticed that the peaks also shifts towards higher angles which indicate the substitution of Zn^{2+} by Mn^{3+} and/or Mn^{4+} ions of smaller ionic radii as discussed by Ahmed [16].

When the Mn dopant ions in the host ZnO lattice is increased, it leads to increased static distortion in the oxygen atom through the Zn(Mn)O coupling. When Zn^{2+} is replaced by Mn^{2+} in the lattice, dispossession of Zn^{2+} from its regular lattice sites and to apparent Zn site vacancies in the lattice occurs. If the valence state is Mn^{3+} or Mn^{4+}then, there is a possibility of Mn–Mn distances reduction. With a regular pattern in increment of the Mn concentration, there should be a uniform shift in the parameters as the Mn concentration increases [7]. However, variations in the trend were observed showing that the difference is not uniform with respect to the Mn concentration. This is an indication of uneven addition of Mn (thus Mn^{2+}, Mn^{3+} or Mn^{4+}).

Comparing this work with that of Senol et al [19] where acetates were used as precursors and samples prepared at temperature of 600 °C for 2 h, Mn_2O_3 was observed as an additional secondary phase at 5% Mn doping concentration. At such a low concentration but higher temperature, fluctuations were observed

in the lattice parameters due to the presence of the Mn replacing Zn ions in the lattice. With the work of Sebayang et al (2020), the peak intensity of the Mn doped ZnO nanoparticles was lower than that of the undoped ZnO and also found to be shifted to higher angles at a maximum doping concentration of 9%. Bilgili [18] observed an increase in the intensity of the diffraction peaks and a shift towards lower angles as the doping concentration increases. In all these cases there were no impurity of secondary peaks observed as the dopant falls below 30% compared this work. The single-phase hexagonal wurtzite structure of ZnO as was observed in the samples conforms to those of Senol et al [19], Sebayang et al [20] and Bilgili [18]. This is an indication that, the procedure and conditions used for this solid state method is unique since at a low temperature of 200 °C and a high doping concentration of above 20% (Mn < 30%), no additional or secondary phase was observed. Since the temperature used for the synthesis is low, application for thin film on flexible substrates such as plastics is possible.

4 Conclusion

The solubility limit for Mn in ZnO synthesized at a temperature of 200 °C is realized at x < 30%. Beyond these dopant concentrations, several secondary peaks are observed in the XRD patterns indicating the presence of secondary phases associated to undissolved acetate other than $Zn_{1-x}Mn_xO$. Shifts in peak positions in the diffraction pattern due to increasing Mn concentration have been observed to be irregular. This is attributed to the different oxidation state of Mn

5 Declarations

5.1 Acknowledgments

I acknowledge with gratitude the co-operation extended by the general office and laboratory staff of the Department of Physics, Legon for the services extended throughout this research period. Special thanks to Mr. Harry Ntumi, the chief technician, Mr. Pamphile Tossou, the assistance chief technician and Evans Adabla, who ensures that all the equipment needed for the experimental work are provided. I am also very grateful to Elena Oti-Padmore and Beatrice Agyapomah for the help with sample characterization on XRD. I take this opportunity to also sincerely thank all the faculty members of the Department of Physics, KNUST, for their support and encouragement.

5.2 Competing Interests

The authors declared that they do not have any conflict of interest in this publication.

How to Cite this Article:

E. N. A. A. Armah, "Solubility of Mn in ZnO Crystallites Synthesized Using Solid State Techniques", *Adv. Nan. Res.*, vol. 3, no. 1, pp. 28-39, Sep. 2020. https://doi.org/10.21467/anr.3.1.28-39

References

[1] O. Masala and R. Seshadri, "Synthesis Routes for Large Volumes of Nanoparticle, Annual Review of Materials Research", vol. 34, no. 1, pp. 41-81, August 2004. DOI: 10.1146/annurev.matsci.34.052803.090949

[2] A. Stadler, "Transparent Conducting Oxides-An Up-To-Date Overview", *Materials*, vol. 5, no. 4, pp. 661–683, 2012.

[3] Y. Caglar, S. Ilican and M. Caglar, *Eur. Phys. J. B 58*, 251, 2007.

[4] H. M. Kim, K. Bae and S. Sohn, "Electronic and Optical Properties of Indium Zinc Oxide Thin Films Prepared by Using Nanopowder Target," *Japanese Journal of Applied Physics*, vol. 50, no. 4, pp. 045801-045805, 2011.

[5] M. Batzill, and U. Diebold, *Prof Surf Sci*, vol. 79, no. 47. 2005.

[6] T. J. Coutts, J. D. Perkins, D. S. Ginley and T. O. Mason, "Transparent Conducting Oxides: Status and Opportunities in Basic Research," *Presented at the 195th Meeting of the Electrochemical Society, Seattle, Washington*, May 2-6, 1999.

[7] R. Saravanan, F. Santhanam and J. L. Berchmans, "Doping level of Mn in high temperature grown $Zn_{1-x}Mn_xO$ studied through electronic charge distribution, magnetization, and local structure", *Chemical Papers*, vol. 66, no. 3, pp. 226–234, 2012. DOI: 10.2478/s11696-011-0129-8

[8] M. Shatnawi, A. M. Alsmadi, I. Bsoul, B. Salameh, M. Mathai, G. Alnawashi, G. M. Alzoubi, F. Al-Dweri, M. S. Bawa'aneh, "Influence of Mn doping on the magnetic and optical properties of ZnO nanocrystalline particles", *Results in Physics*, vol. 6, pp. 1064–1071, 2016.

[9] G. Voicu, O. Oprea, B. S. Vasile and E. Andronescu, "Photoluminescence and Photocatalytic Activity of Mn-Doped ZnO Nanoparticles". *Digest Journal of Nanomaterials and Biostructures*, vol. 8, no. 2, pp. 667-675. 2013.

[10] P. Thamaraiselvan, M. Venkatachalam, M. Saroja, P. Gowthaman, S. Ravikumar and S. Shankar, "Structural, morphological, optical and magnetic characterization of Mn Doped ZnO", *International Journal of Multidisciplinary Research and Development*, volume 3; Issue 3; Page No. pp. 102-104, 2016.

[11] N. Singh, S. Mittal, K. N. Sood, Rashmi, P. K. Gupta, "Controlling the Flow of Nascent Oxygen Using Hydrogen Peroxide Results in Controlling the Synthesis of ZnO/ZnO_2", *Chalcogenide Letters*, vol. 7, no. 4, pp. 275-281, April 2010.

[12] U. V. Desnical, "Doping Limits in Il-VI Compounds-Challenges, Problems and Solutions", *Prog. Crystal Growth and Charact.*, vol. 36, no. 4. pp. 291-357, Elsevier Science Ltd., Great Britain, 1998.

[13] M. Wang, A. Debernardi, Y. Berencén, R. Heller, C. Xu, Y. Yuan, Y. Xie, R. Böttger, L. Rebohle, W. Skorupa, M. Helm, S. Prucnal and S. Zhou, "Breaking the Doping Limit in Silicon by Deep Impurities", *Physical Review Applied*, vol. 11, 054039, 2019.

[14] D. Lançon, G. J. Nilsen, A. R. Wildes, K. Nemkovski, P. Huang, D. Fejes, H. M. Rønnow and A. Magrez, "MnO nanoparticles as the cause of ferromagnetism in bulk dilute Mn-doped ZnO", *Appl. Phys. Lett*. vol. 109, 252405, pp. 1-5, 2016. DOI: 10.1063/1.4972956

[15] J. Marquina, J. Mart´ın, J. Luengo, F. Vera, L. Roa, G. E. Delgado, F. Rodr´ıguez, C. Renero-Lecuna, R. Valiente and J. Gonz´alez, "Structural refinement, photoluminescence and Raman spectroscopy of Wurtzite Mn-doped ZnO pellets", *Revista Mexicana de F´ısica,* vol. 63, pp. 32–39, 2017.

[16] S. A. Ahmed, "Structural, optical, and magnetic properties of Mn-doped ZnO samples", *Results in Physics*, vol. 7, pp. 604–610, 2017.

[17] H. Mobarak, S. C. Paul, M. S. Islam, S. Akter and K. Sohag, "Study on the Frequency and Temperature Dependent Electrical Properties of MnO and PbO Doped ZnO Nanoceramics," *J Adv Chem Eng.*, vol 8, no. 1, 2018. DOI: 10.4172/2090-4568.1000183

[18] O. Bilgili, "The Effects of Mn Doping on the Structural and Optical Properties of ZnO," *ACTA PHYSICA POLONICA A,* vol. 136, no. 3, pp. 460-465, 2019. DOI: 10.12693/APhysPolA.136.460

[19] S. D. Senol, E. Ozugurlu and L. Arda, "Synthesis, structure and optical properties of (Mn/Cu) co-doped ZnO nanoparticles", *Journal of Alloys and Compounds*, 822, pp. 1-12, 2020. DOI: 10.1016/j.jallcom.2019.153514

[20] P. Sebayang, C. Kurniawan, R. Y. Lubis, I. Priyadi, M. N. Nasruddin and D. Aryanto, "Investigation of Microstructure and Magnetic Properties of Zn1-xMnxO and Zn0.98-xMnxFe0.02O (x = 0, 0.05, and 0.09) prepared by Solid-state Reaction Method**,"** *Makara Journal of Science*, vol. 24, no. 2, pp. 95-100, June 2020**.** DOI: 10.7454/mss.v24i1.11914

[21] E. N. A. Armah, F. K. Ampong, M. Egblewogbe, H. A. Koffi, F. Boakye, J. K. A. Amuzu, R. K. Nkum, Solubility of Mn in ZnO Nanocrystallites using Wet Chemical Synthesis, *Adv. Nan. Res.;* Vol. 2, no. 1, pp: 53-61, November 2019. DOI: https://doi.org/10.21467/anr.2.1.53-61

[22] A. N. Fauzana, B. Z. Azmi, M. G. M. Sabri, W. R. W. Abdullah and M. Hashim, "Microstructural and Nonlinear Electrical Properties of ZnO Ceramics with Small Amount of MnO_2 Dopant", *Sains Malaysiana*, vol. 42, no. 8, pp. 1139–1144, 2013.

[23] M. C. Morris, H. F. McMurdie, E. H. Evans, B. Paretzkin, H. S. Parker, N. C. Panagiotopoulos, and C. R. Hubbard, "Standard X-ray Diffraction Powder Patterns Section 18 Data for 58 Substances, International Centre for Diffraction Data", Library of Congress Catalog Card Number: 53-61386, Nat. Bur. Stand. (U.S.), Monogr. 25-Sec. 18, pp. 110, 1981.

[24] A. G. Ali, F. B. Dejene and H. C. Swart, "Effect of Mn doping on the structural and optical properties of sol-gel derived ZnO nanoparticles", *Cent. Eur. J. Phys.* vol. 10, no. 2, pp. 478-484, 2012. DOI: 10.2478/s11534-011-0106-4

[25] T. M. Dhruvashi and P. K. Shishodia, "Ferromagnetism in sol-gel derived ZnO:Mn nanocrystalline thin films", *Adv. Mater. Lett.*, vol. 7, no. 2, pp. 116-122, 2016. DOI 10.1007/s13204-012-0089-5

[26] G. Voicu, O. Oprea, B. S. Vasile and E. Andronescu, "Photoluminescence and Photocatalytic Activity of Mn-Doped ZnO Nanoparticles," *Digest Journal of Nanomaterials and Biostructures*, vol. 8, no. 2, pp. 667-675, 2013.

[27] V. D. Mote, J. S. Dargad, and B. N. Dole, "Effect of Mn Doping Concentration on Structural, Morphological and Optical Studies of ZnO Nano-particles", *Nanoscience and Nanoengineering* vol. 1, no. 2, pp. 116-122, 2013. DOI: 10.13189/nn.2013.010204

[28] B. Goswami and R. Singha, "Effect of Mn Doping on Optical Properties of ZnO Nanoparticles". *IJIRSET*, vol. 4, no. 4, pp. 2577, 2015. DOI: 10.15680/.2015.0404073

[29] E. M. Abrishami, S. M. Hosseini, A. E. Kakhki, A. Kompany and M. Ghasemifard, "Synthesis and Structure of Pure and Mn-Doped Zinc Oxide Nanopowders", *International Journal of Nanoscience* vol. 9, nos. 1 and 2, pp. 19-28, 2010. DOI: 10.1142/S0219581X1000648X

[30] S. Deka and P. A. Joy, "Synthesis and magnetic properties of Mn doped ZnO nanowires", *Solid State Communications*, vol. 142, pp. 190-194, 2007.